33rd Annual International Conference of the IEEE EMBS
Boston, Massachusetts USA, August 30 - September 3, 2011

Electromagnetic Analysis of an RF Rectangular Resonant Cavity Applicator for Hyperthermic Treatment using Whole-Body Voxel Human Model of Japanese Adult Male

Yutaka Tange, *Member, IEEE*, Kosuke Yabumoto, and Yasushi Kanai, *Member, IEEE*

***Abstract*— The numerical whole-body voxel human model (numerical model) developed by National Institute of Information and Communications Technology (NICT) was assumed and hyperthemic treatment using radio-frequency wave was investigated. We assumed 51 different human tissues and organs with 2-mm spatial resolution in the numerical model, inserted it into the resonant cavity applicator, and Maxwell's equations were solved by FDTD method with variable mesh. We obtained the realistic energy patterns for a deep-seated tumor as compared to those obtained in our previous studies.**

I. Introduction

CANCER is the uncontrolled growth and spread of cells. It can affect almost any part of the body. The growths often invade the surrounding tissues and even metastasize to distant sites [1]. Therefore, it is desirable to remove the cancer from the human body as soon as possible.

Hyperthermia is a cancer therapy that focuses on the difference in heating sensitivity between a tumor and non-tumor cells. In comparison to non-tumor cells that live up to 44°C, the tumor dies from 42.5°C upward. By using electromagnetic energy, the tumor cells are heated up to a temperature at which they die.

Heating devices for noninvasive hyperthermia such as radiofrequency and microwave heating applicators [2] have already been developed. However, deep-seated tumors cannot be sufficiently heated by these devices because of the complex human tissues and the cooling effect caused by the blood flow. A phased array system [3] with multiple antennas can focus the electromagnetic energy on a deep-seated tumor. However, it is very difficult to determine the optimum amplitude and phase of power for each patient. In recent experimental studies, very small implants [4] and magnetic fluids have been developed; they can heat a tumor using an inductive heating applicator. The question is how to focus the energy on local regions containing the tumor in the human body. A numerical study on a new heating technique—the annular-shaped inductive aperture-type applicator—has been reported [5]. In the report, a cylindrical body with a fat layer was used. Although heat generation was possible in deep regions of the body, it was noted that the heating occurred between the muscle and the fat layer.

We have already reported a reentrant cavity applicator that targets deep-seated tumors [6]: the deep region of a small disk-shaped dielectric phantom could be heated. We have also developed an RF rectangular resonant cavity applicator for a larger model with deep-seated tumors [7], [8]. By optimizing the positions of multiple antennas in the applicator, we heated the deep interior of the phantom [9]. In order to realize local heating, conductive caps were attached to the dielectric phantom. As a result, we could heat the selective region. Before the clinical stage, it is necessary for us to model the components of a human body accurately, e.g., blood flow, human organs, and the fat layer.

In this paper, we will investigate the possibility of heating the deep region of a numerical human model using an RF rectangular resonant cavity applicator for deep-seated tumors before the modeling of tumors. Simulation results show that this applicator can heat deep region.

II. Resonant Cavity Applicator

The experimental setup used in our study is illustrated in Fig. 1. The cavity applicator consists of copper plate. In the cavity applicator, the heated object is placed on a wooden table. Loop antenna is placed beside the object at the center of the applicator in the x-direction. The electric power is applied to the antenna set inside the applicator. Then, the electric and magnetic fields occur in the cavity. In order to realize deep heating, the lowest resonant frequency (TE011 mode) is used. In this study, the electric field strength along x direction of the cavity does not change.

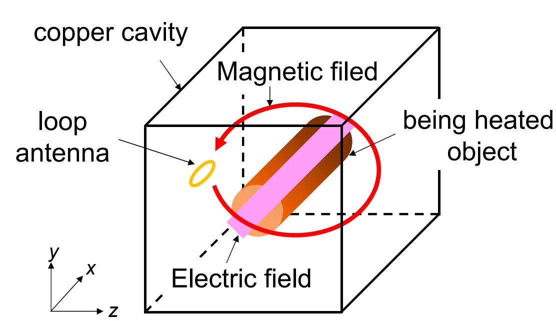

Fig. 1. Arrangement of a rectangular resonant cavity applicator.

Manuscript received Aril 15, 2011.

Yutaka Tange and Kosuke Yabumoto are with Maizuru National College of Technology, Maizuru 625-8511, Japan. (phone: +81-773-62-8970; fax: +81-773-62-8970; e-mail: tange@maizuru-ct.ac.jp).

Yasushi Kanai is with Niigata Institute of Technology, Kashiwazaki 945-1195, Japan.

III. ELECTROMAGNETIC EQUATION FOR CALCULATION

For analyzing the electromagnetic field in the cavity, we solved Maxwell's equations using the three-dimensional finite-difference time-domain (FD-TD) method [10].

$$\nabla \times \mathbf{E} = -\mu \frac{\partial \mathbf{H}}{\partial t}, \ \nabla \times \mathbf{H} = \sigma \mathbf{E} + \varepsilon \frac{\partial \mathbf{E}}{\partial t} \qquad (1)$$

where μ, σ, and ε represent the permeability, electrical conductivity, and permittivity, respectively. Note that the cavity walls were assumed to be perfect electrical conductors. In the electromagnetic analysis, we first derived the resonant frequencies in the cavity. Then, the electromagnetic energy at the lowest resonant frequency was applied. After analyzing the fields, the object that was heated by the electromagnetic energy was examined using the following formula.

$$W = \frac{1}{2T}\sigma \int |\mathbf{E}|^2 dt \qquad (2)$$

IV. ANALYSIS MODELS

The Numerical Whole-Body Voxel Human Model

The numerical whole-body voxel human model (numerical human model) used in our study, which was developed by National Institute of Information and Communication Technology, is illustrated in Fig. 2 [11], [12]. This model was invested with 51 human tissues and organs with ID and made by using voxel data. The adult male model consists of the voxel data of 320 × 160 × 866 with spatial resolution 2-mm. The electrical parameters used in the calculation are listed in Table I [13].

As shown in Fig. 2, the liver tumor is targeted in our study, therefore, only the body (length 580 mm) surrounded with red broken line between shoulder and hip was inserted into the resonant cavity applicator. In this study, the possibility of heating the deep region without liver tumors was investigated in the analysis.

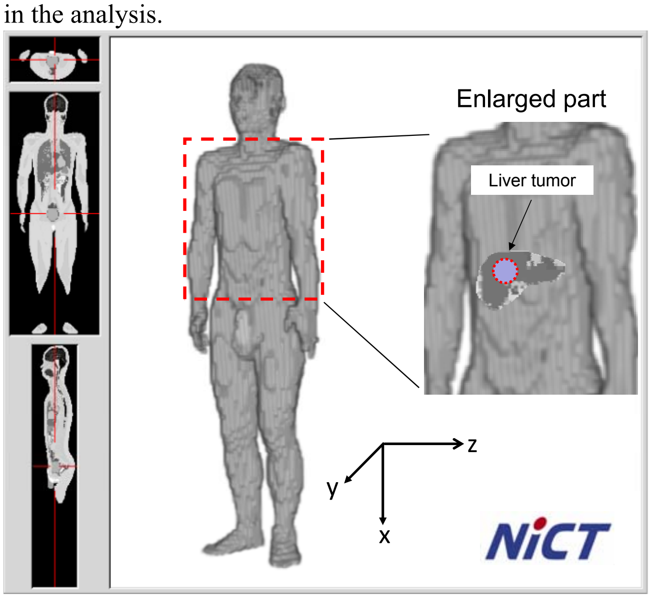

Fig. 2. Realistic high–resolution whole-body voxel model of Japanese adult male.

TABLE I
TYPICAL ELECTRIC PROPERTIES [13]

Tissue	ε_r	σ [S/m]
Blood	76.8	1.23
Bone Cancellous	27.6	0.17
Bone Cortical	15.3	0.06
Bone Marrow Infiltrated	14.3	0.16
Bone Marrow Not Infiltr	6.5	0.02
Cartilage	55.8	0.47
Colon(Large Intestine)	81.8	0.68
Fat(Mean)	12.7	0.07
Gall Bladder	79.0	1.01
Gall Blad Bile	95.0	1.54
Heart	90.8	0.73
Kidney	98.1	0.81
Liver	69.0	0.49
Lung	49.4	0.43
Muscle	66.2	0.73
Nerve(Spinal chord)	47.3	0.34
Skin	69.4	0.51
Small Intestine	96.5	1.66
Spleen	90.7	0.80
Stomach Esop Duodenum	77.9	0.90
Thyroid Thymus	68.8	0.79
Trachea	53.0	0.55
Pancreas	66.2	0.73

A. *Cavity Applicator Inserted in the Human Model*

Fig. 3 shows the analysis model of the resonant cavity applicator inserted in the numerical human model. In order to assume the clinical stage, the cavity was designed to have two holes on the wall so as to be inserted in the human model. The Mur's 1st order was applied to absorb the leak of electric and magnetic fields in front of the insertion holes. A set of exciting sources with opposite phase was placed in the cavity because electromagnetic fields with opposite phase are known to be capable of heating the deep region from the effect of superposition [7].

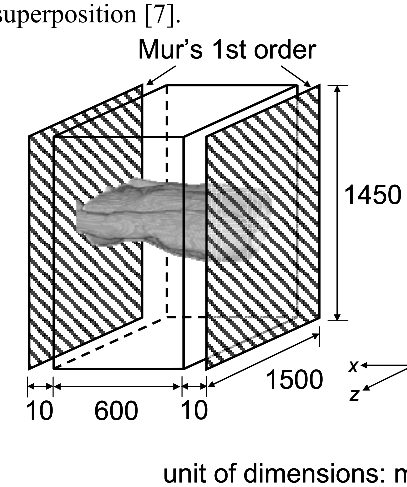

Fig. 3. Numerical structure of the cavity inserted in the human model.

V. VARIABLE MESH

FD-TD method is capable of changing the mesh size in the analysis area. It was found that the discretization error can be estimated to the order of $O(\delta x^1)$ of the mesh size [14]. As a result, the amount of memory used and the calculation time were greatly reduced.

If the model is divided into 2-mm in spatial resolution, a lot of memory and calculation time will be needed. For example, the use of variable mesh can reduce computer memory to 4 [GB], while 10 [GB] is needed without it. It was found that the variable mesh made calculation stable in large-scale computer analysis.

VI. CALCULATED RESULTS AND DISCUSSIONS

In this study, the cylindrical phantom (ϕ 300mm × 500 mm length) and the numerical human model are used to compare the two groups of the electromagnetic distributions due to the difference in the shapes of the models.

A. Case in which the Cylindrical Phantom is Used

Fig. 4 shows the resonant frequency curve of the cavity applicator with the cylindrical phantom which is equal in volume to the human model. As shown in Fig. 4, it was found that the resonant frequency was 86.7 MHz at the peak point. In addition, it described a smooth curve.

Fig. 5 shows the electromagnetic energy of the phantom. In Figs. 5(a)-(c), it is observed that energy is focused on the central region of the phantom and also strongly distributed to the surface region. Therefore, it may be said that this applicator can heat the deep-seated tumor. However, according to the thermal analysis, it may be necessary to reduce the surface temperature by using a cooling system such as water bolus.

From these results, it is presumed that the energy is concentrated on the deep region of the numeral human model.

B. Case in which the Numerical Human Model is Utilized

Fig. 6 shows the resonant frequency of the cavity applicator inserted in the human model. As shown in Fig. 6, the resonant frequency is 88.8MHz at the peak point. Compared with the frequency of the cylindrical phantom, the curve changed in this case because of the effect of the shape of the model.

Fig. 7 shows the electromagnetic energy of the human model. In Figs. 7(a)-(b), the electromagnetic energy is concentrated on the deep region of the model. Especially, the energy is focused on the pancreas. Moreover, it is observed that the energy is slightly focused on targeting the liver region. From our previous results [15], we reflected on the concentration of the energy on the regions with low conductivity, for example, the liver and lung regions. These results show their dependence on both the conductivity and the size of the organs. So, it may be necessary to investigate the temperature distributions by using the heat-transfer analysis.

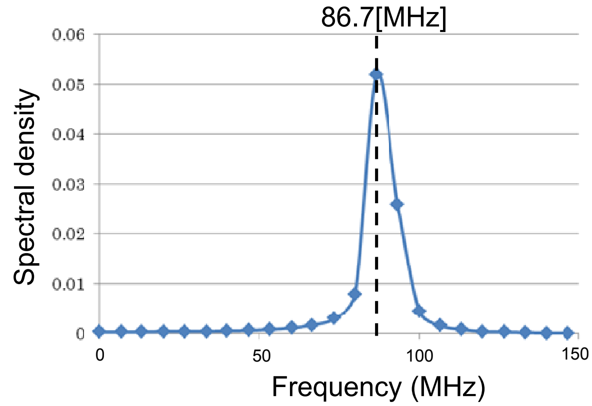

Fig. 4. Resonant frequency curve of the cavity applicator with the cylindrical phantom.

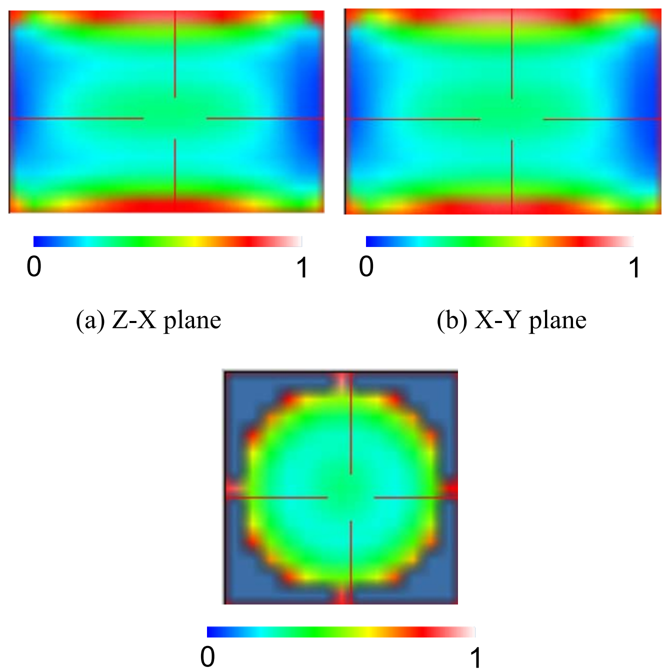

(a) Z-X plane (b) X-Y plane

(c) Y-Z plane

Fig. 5. Normalized electromagnetic energy of the cavity applicator inserted in the cylindrical phantom.

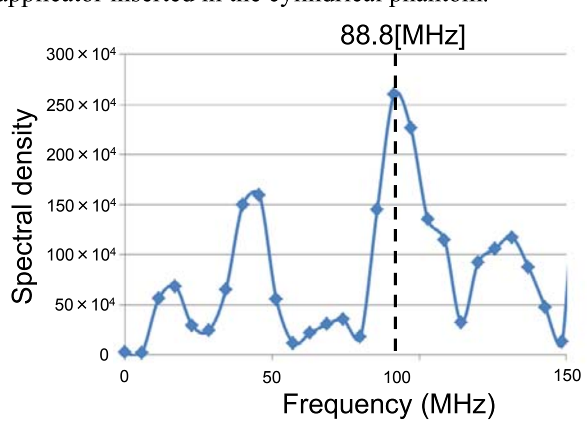

Fig. 6. Resonant frequency curve of the cavity applicator with the human model.

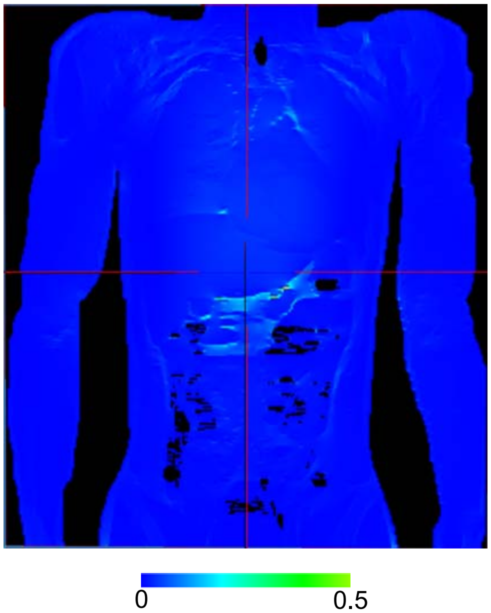

(a) Z-X plane

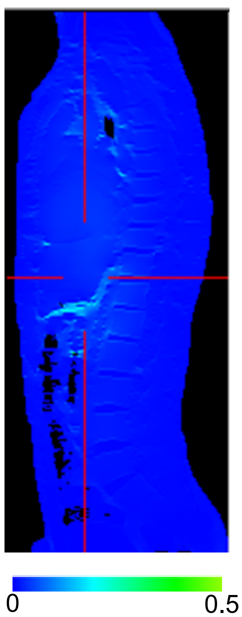

(b) X-Y plane

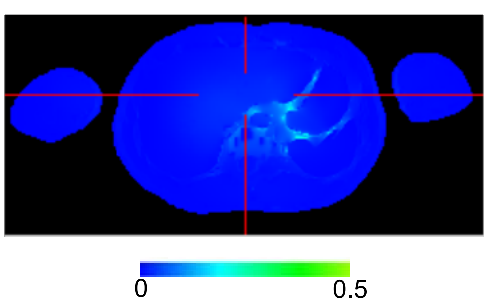

(c) Y-Z plane

Fig. 7. Normalized electromagnetic energy of the numerical human model.

VII. Conclusion

In this study, the electromagnetic patterns of an RF resonant cavity applicator for hyperthermia targeting liver tumor have been investigated numerically. Before the modeling of tumors, the numerical whole-body voxel human model, which was developed by National Institute of Information and Communication Technology, without liver tumor was modeled and analyzed. We obtained the realistic energy patterns for deep heating as compared to those obtained in our previous study.

References

[1] World Health Organization web site [Online]. Available: http://www.who.int/cancer/en/.

[2] K. Ito and K. Saito, “Microwave antennas for thermal therapy,” *Japanese Society for Thermal Medicine*, vol. 23, no. 1, pp. 23–30, Mar. 2007.

[3] N. Siauve, L. Nicolas, C. Vollaire, A. Nicolas, and J. A. Vasconcelos, “Optimization of 3-D SAR distribution in local RF hyperthermia,” *IEEE Trans. on Magn*., vol. 40, no. 2, pp. 1264–1267, Mar. 2004.

[4] Y. Kotsuka and H. Okada, “Development of small and high efficiency implant for deep local hyperthermia,” *Jpn. J. Hyperthermic Oncol.*, vol. 19, no.1, pp. 11–22, Mar. 2003.

[5] H. Kato, M. Kuroda, K. Shibuya, and A. Kanazawa, “Focused deep heating with an inductive type applicator,” *Thermal Medicine*, vol. 23, no. 3, pp.133–143, Oct. 2007.

[6] K. Kato, J. Matsuda, and Y. Saitoh, “A re-entrant type resonant cavity applicator for deep-seated hyperthermia treatment,” *Proc. Annual Int’l Conf. of the IEEE Eng. in Medicine and Biology Society*, vol. 11, pp. 1712–1713, Nov. 1989.

[7] S. Soeta, S. Yokoo, M. Shimada, Y. Kanai, and J. Hori, “Eigenmode analysis of a parallelepiped resonator for hyperthermic treatment by using FD-TD method,” *10th Niigata Branch Regional Meeting of IEE Japan*, III-21, Nov. 2001 (in Japanese).

[8] Y. Tange, Y. Kanai, and Y. Saitoh, “Analysis and development of a radio frequency rectangular resonant cavity applicator with multiple antennas for a hyperthermic treatment,” *IEEE Trans. on Magn.,* vol. 41, no. 5, pp. 1880–1883, May 2005.

[9] Y. Tange, Y. Kanai, Y. Saitoh, and T. Kashiwa, “New heating characteristics of a radio frequency rectangular resonant cavity applicator using various antennas for hyperthermic treatment,” *ACES Journal*, vol. 22, no. 2, pp. 269–276, July 2007.

[10] D. Sullivan, “Three-dimensional computer simulation in deep regional hyperthermia using the finite-difference time-domain method,” *IEEE Trans. on Microwave Theory Tech.*, vol. 38, no. 2, pp. 204–211, Feb. 1990.

[11] T. Nagaoka, S. Watanabe, K. Sakurai, E. Kunieda, S. Watanabe, M. Taki and Y. Yamanaka, “Development of realistic high-resolution whole-body voxel models of Japanese adult male and female of average height and weight, and application of models to radio-frequency electromagnetic-field dosimetry,” *Physics in Medicine and Biology*, vol.49, pp.1-15, 2004.

[12] National Institute of Information and Communications Technology [Online]. Available: http://www2.nict.go.jp/y/y224/bio/data/index_e.html

[13] Federal Communications Commission web site [Online]. Available: http://www.fcc.gov/fcc-bin/dielec.sh.

[14] Y. Kanai and K. Sato, “Automatic mesh generation for 3D electromagnetic field analysis by FD-TD method,” *IEEE Trans. on Magn*., vol. 34, no. 5, pp. 3383–3386, Sep. 1998.

[15] Y. Kanai, T. Tsukamoto, Y. Saitoh, M. Miyakawa, and T. Kashiwa, “Analysis of a hyperthermic treatment using a reentrant resonant cavity applicator for a heterogeneous model with blood flow,” *IEEE Trans. on Magn*., vol. 33, no. 2, pp. 2175–2178, Mar. 1997.